UNIVERSITY OF SOUTHAMPTON

DEPARTMENT OF SHIP SCIENCE

FACULTY OF ENGINEERING AND APPLIED SCIENCE

THE DESIGN, CONSTRUCTION AND CALIBRATION OF A WAVE BUOY FOR SHIP MODEL TESTS IN OPEN WATER

J.F. Wellicome, P.Termarel, A.F.Molland, J.Cic and D.J.Taunton

Ship Science Report No. 112
October, 1999

THE DESIGN, CONSTRUCTION AND CALIBRATION OF A WAVE BUOY FOR SHIP MODEL TESTS IN OPEN WATER

J.F. Wellicome, P. Temarel, A.F. Molland, J. Cic and D.J. Taunton

Ship Science Report No. 112

University of Southampton

October, 1999

CONTENTS

1 INTRODUCTION 4

2 THE CONSTRUCTION OF THE BUOY 4

3 BUOY DEPLOYMENT AND OPERATION 5

4 CALIBRATION OF THE BUOY 6

5 ANALYSIS OF BUOY DATA FROM TESTS IN OPEN WATER 7

6 MEASURMENTS OF WAVE SPECTRA 9

6.1 Frequency Spectra from Power Spectral Density of Acceleration Data (method (a))...9
6.2 The estimation of spectral directional properties (methods (b) and (c))..... 10

7 CONCLUSIONS 12

APPENDIX 1: ESTIMATION OF BUOY MOTIONS RELATIVE TO DATUM DIRECTIONS BASED ON COMPASS ZERO HEADING.

APPENDIX 2: IDENTIFICATION OF WAVE SPECTRAL DETAILS

APPENDIX 3: BUOY INSTRUMENTATION

Table 1: Buoy calibration data

Figure 1: Wave buoy Configuration
Figure 2a: Buoy Heave Transfer Function
Figure 2b: Buoy Roll Transfer Function
Figure 2c: Buoy Pitch Transfer Function
Figure 2d: Buoy Roll T.F./ Buoy Pitch T.F.
Figure 3a: Acceleration Spectral Density
Figure 3b: Amplitude Spectral Density
Figure 4a: Heave Auto-correlation
Figure 4b: Pitch Auto-correlation
Figure 4c: Roll Auto-correlation
Figure 5: Roll-Pitch Phase
Figure 6: Mean Direction at Each Frequency Band
Figure 7a: Pitch/ Heave Amplitude
Figure 7b: Roll/Heave Amplitude
Figure 8: Spreading Function Integral

NOMENCLATURE

η	Wave elevation [m]
ζ	Wave amplitude [m]
$S(\varpi_n, \theta_m)$	Directional spectral density for the wave elevation
$D_n(\theta)$	Spreading Function
μ	Heading angle [deg]
θ	Component wave angle [deg]
ω	Wave frequency [Hz]
Fn	Froude Number, $[u/\sqrt{gL}]$
u	Velocity $[ms^{-1}]$
FFT	Fast Fourier transform
TF	Transfer function
g	Acceleration due to gravity $[9.80665\ ms^{-2}]$

1 INTRODUCTION

The need to measure sea state in open water experiments, aimed at obtaining response data for models of fast multihull vessels in oblique seas, prompted the design and construction of a simple wave buoy based on a circular lifebelt. The buoy is fitted with three accelerometers mounted on top of the lifebelt to measure the buoy heave, pitch and roll responses to waves, together with a flux-gate compass to monitor buoy heading. Power supplies to the instrumentation and output signals from them are carried along a 50m umbilical cable to the support boat accompanying the model tests.

The rationale for constructing a special purpose wave buoy was twofold:

1. The buoy would always be available at short notice and be easily transported to test sites.

2. The buoy could be designed to measure the relatively short wavelengths appropriate to tests on the models concerned. Since the models were 4.5m long, the buoy should be capable of measuring waves down to about 2m in length. Descriptions of the catamaran models used in the tests are given in Refs. 1 and 2.

In principle, the buoy is capable of measuring a directional wave spectrum, at least to the extent of estimating an approximate wave spreading function and mean wave direction, together with a one dimensional power spectrum.

The buoy has been successfully calibrated and used for wave measurements in Southampton Water in association with motions measurements of a fast catamaran model.

2 CONSTRUCTION OF THE BUOY

As stated in the introduction, the wave buoy is based on a lightweight circular lifebelt. The general layout of the buoy can be seen in Fig. 1. Upwind of the buoy is a drogue intended to slow down the buoy drift to leeward, whilst downwind of the buoy is a 50m long umbilical consisting of four light multi-core power/signal cables and a polypropylene tow line tied together at approximately 2m intervals. Foam floats were tied to the cable at about 5m intervals. 12-volt dc power supplies and data logging equipment at the far end of the umbilical are carried in the support boat.

In practice it was found that the support boat drifted down wind slightly faster than the buoy itself, so that the buoy deployed directly to windward of the boat with the umbilical extended fully, but not tightly. The buoy thus deploys naturally in a way that can be considered ideal.

Two wooden beams across the buoy support a cradle to carry the fluxgate compass in a waterproof box suspended in the centre of the buoy ring. A ballast weight, sufficient to load the buoy to a waterline at mid depth of the ring, is mounted on top of the compass cradle.

The umbilical carries a small weight close to the buoy to ensure that the cables lead downwards from the buoy before streaming away towards the support boat.

The outside diameter of the buoy ring is 650mm and the accelerometers are mounted at 120 degree intervals round the ring at a radius of 245mm. Details of the accelerometers, compass and data acquisition are given in Appendix 3.

3 BUOY DEPLOYMENT AND OPERATION

As a general rule, model trials in Southampton Water were conducted over a four or five hour period commencing about one hour before 1st high water. A typical test procedure commenced with a model test run followed by a buoy deployment. The intention was to re-deploy the buoy following every third or fourth model run thereafter. This pattern of operation was not ideal. It would have been preferable to continuously monitor wave conditions throughout the test period. However, this would have required the use of a second support boat and additional data acquisition equipment and personnel. As it was, there were occasions when significant changes of wave conditions occurred between buoy deployments.

It should be pointed out that during a model test run the support boat followed the model at speeds of the order of 4 m/s in order to monitor model speed. A typical test run was of 5 or 6 min duration and covered some 1200 m. The wave buoy was deployed in the centre of the intended test area, but it was difficult to ensure the model remained in that area throughout the test period.

During buoy deployment wind speed was monitored using a simple "Ventimeter" yachtsman's wind gauge. Wind direction and the cable lead angle from the support boat to the buoy were measured with a hand bearing compass. Broadly, the wind direction and mean cable angle agreed within 5 to 10 degrees. When measuring waves, with a slack umbilical, the buoy yawed slowly through some 20 degrees either side of the mean buoy heading. The fluxgate compass measured over a range of approximately 45 degrees either side of an arbitrary zero set from the support boat when the buoy is fully deployed. This is sufficient to record the buoy yaw motion, but gave no direct indication of mean buoy heading. It was found that if the buoy was towed slowly the umbilical extended in a straight line from boat to buoy and yaw reduced to a few degrees only. Thus, once a set of wave measurements had been acquired, the buoy was towed slowly to relate fluxgate compass output to a known magnetic heading.

The observed buoy yaw motion during wave measurement was aperiodic and slow, taking about a minute from one extreme angle to the other. Superimposed on this slow motion was a wave related high frequency yaw motion of much smaller amplitude. There is some doubt of the response of the compass to high frequency yaw motions. Consequently it is desirable to filter such motions from the compass output and to retain data for slow heading changes only.

4 CALIBRATION OF THE BUOY

Prior to the construction of the buoy some theoretical responses were investigated for a number of possible buoy geometries, seeking a configuration that would have a flat, unit response operator in both pitch and heave over the range of wave frequencies of interest. The ring configuration appeared to satisfy this requirement. It should be pointed out, however, that neither the fluxgate compass nor the umbilical cable was modelled in the theoretical calculations.

The buoy as finally constructed was calibrated in the Lamont tank at the University of Southampton, moored in its intended orientation to the dominant wave direction (along the tank centreline in this case) and also at a heading of 90 degrees to this direction. The first orientation provided heave and pitch calibration data and the second provided additional roll calibration data. Because of the restricted water depth in the towing tank and also its short length, the maximum wavelength that could sensibly be generated was only 5m (corresponding to a wave frequency of 0.55 hz). The shortest wavelength was 1.5m, or about twice the outer diameter of the buoy (corresponding to a wave frequency of 1.1 hz).

Measured catamaran model responses indicate the desirability of measuring wave data for wavelengths up to about 4 times model length, or about 20m (corresponding to a wave frequency of 0.3 hz). To date it has not been possible to calibrate the buoy in a facility permitting the generation of such waves. However, the buoy heave response operator clearly tends towards unity in long waves and this is readily apparent in the wave lengths actually tested.

Table 1 gives transfer functions for buoy responses in regular waves, based on RMS values of buoy accelerations, as tested in the Lamont tank. These results are shown graphically in Fig 2. The heave response of the buoy is more or less as expected, being a flat response at a few percent above wave amplitude at low frequencies and falling off at frequencies above 1.0 hz. The roll and pitch responses appear to be quite large at low frequencies and to fall to values comparable with wave slope as frequency increases. This was not expected from the preliminary theoretical studies and seems to indicate larger rotary motions than were apparent from visual observation. However, the indicated pitch and roll responses seem qualitatively to match measurements made in open water in irregular waves. At present there is no obvious explanation for these calibration characteristics.

Qualitatively the roll and pitch results are similar. If the pitch transfer function results are shifted by 0.1 hz to lower frequencies the ratio of roll transfer function to pitch transfer function is reasonably constant over the range of frequencies tested. The roll T.F. being, on average, about 90% of the pitch T.F. This is shown in Fig 2d. The calibration analysis assumed that the accelerometers were placed exactly at 120 degree intervals round the buoy. In fact measurement of the actual positions of the accelerometers shows the precise locations to differ slightly from this requirement in such a way as to reduce the roll signal and increase

the pitch signal from the buoy. The true roll and pitch responses could in fact be equal or nearly so. This possibility is made use of in estimating the directional properties of a wave spectrum.

Ideally, it would be desirable to have phase information for the buoy motions relative to the wave passage. Unfortunately the calibration data was not of sufficiently good quality to allow the estimation of phase.

5 ANALYSIS OF BUOY DATA FROM TESTS IN OPEN WATER

The elevation of the sea surface can be represented by an equation of the form:

$$\eta = \sum_n \sum_m \alpha_{n,m} \cos[k_n x \cos\vartheta_m + k_n y \sin\vartheta_m - \omega_n t + \phi_{n,m}] \quad \ldots\ldots (1)$$

where

ω_n = Component wave frequency (rad/s)
k_n = Component wave number (1/m)
ϑ_m = Component wave direction
$\alpha_{n,m}$ = Component wave amplitude (m)
$\phi_{n,m}$ = Random component phase angle (rad)

In this equation the x-axis is along the reference wave direction $\vartheta_m = 0$, which will be taken to be the mean direction of the buoy longitudinal axis.

The directional spectral density for the wave elevation, $S(\omega_n, \vartheta_m)$, can be defined in terms of the component wave amplitudes by the equation:

$$S(\omega_n, \vartheta_m)\delta\vartheta_m\delta\omega_n = 1/2(\alpha_{n,m})^2 \quad \ldots\ldots (2)$$

Because the wave buoy provides rather limited information about the sea surface, in particular because the buoy measures data at only one point in space, the directional spectrum will be simplified to the form:

$$S(\omega_n, \vartheta_m) = S(\omega_n).D_n(\vartheta_m - \mu_n) \quad \ldots\ldots (3)$$

Here $D_n(\vartheta_m - \mu_n)$ is a spreading function assumed to be symmetric about a given mean wave direction μ_n and having the property that

$$\int_{-\pi/2}^{\pi/2} D_n(\vartheta)d\vartheta = 1.0 \quad \ldots\ldots (4)$$

The choice of spreading function is somewhat arbitrary. A convenient and common choice is to use the form given in equation (A2.8):

$$D(\vartheta') = a\cos^{2p}(\vartheta') \quad : \qquad \frac{-\pi}{2} < \vartheta' < \frac{\pi}{2} \qquad \ldots(\text{A } 2.8)$$

The objective of the buoy analysis procedure is to determine $S(\omega_n), \mu_n$ *and* $D_n(\vartheta)$ for each wave frequency present in the spectrum. This is accomplished by examining the auto- and cross-correlations of wave elevation and the wave slopes along the reference wave direction and across it. The wave elevation and slopes are determined from the buoy heave, pitch and roll responses via the buoy calibrations. The auto- and cross- correlations are determined from fast Fourier transforms of the time histories of the buoy motions. The details of the identification of wave spectral information are set out in Appendix 2.

Because of changes of buoy heading (due to yaw effects), the instantaneous accelerometer records do not directly give pitch and roll data about the reference buoy direction. It is necessary to convert the acceleration data into vertical displacements at the accelerometers and subsequently, by a suitable co-ordinate rotation allowing for the instantaneous buoy heading, to compute the buoy pitch and roll about the reference axes. This process is detailed in Appendix 1.

The use of a fluxgate compass to monitor buoy heading is not ideal. The output voltage from the compass is somewhat unsteady, does not react correctly to rapid changes of heading and is sensitive to buoy motions (particularly pitch and roll). In order to obtain a useable output from the compass, the raw signal was heavily smoothed digitally by performing an FFT and retaining only those frequency components below that of the longest wave of interest from the viewpoint of model motions. The inversion of the truncated FFT yields a slowly varying yaw motion similar to that observed visually.

In converting accelerometer data into vertical displacements the method adopted is to perform an FFT of the accelerometer data, to remove any slow drift by deleting frequency components below the minimum frequency of interest from the point of view of catamaran model responses, to remove high frequency components associated with signal noise and to divide the remaining components by frequency squared. Predicted vertical displacements were found by inverting the truncated FFT. If the low frequency components are not removed the buoy can appear to be displaced several meters from the mean sea level. Once they are removed the buoy appears to oscillate, correctly, about a zero mean level.

Analysis of wave buoy data has been carried out in three different ways:

a) Buoy accelerometer data was used directly to calculate the power spectral density of buoy heave acceleration as a route to estimating $S(\omega_n)$ by itself.
b) Smoothed time series data of accelerometer displacements and compass heading, as outlined above, were converted to time series data for buoy heave, pitch and roll referred to the compass zero direction, as set out in Appendix 1. The FFT of auto- and cross-

correlations of the motions required for the estimation of wave spectral density, mean wave direction and spreading function (as set out in Appendix 2) were found from these time series.

c) An analysis using the mean value of compass heading as a constant heading angle replaced the co-ordinate transformation on a point by point basis of method b). In this case, since the effects of yaw rate and yaw acceleration are suppressed, the coefficients of the auto- and cross-correlations can be obtained directly from the accelerometer acceleration data without the need to construct time series of accelerometer displacements.

The analysis procedures outlined above can be carried out using the mathematical routines available within the DASY*Lab* software used for all data acquisition purposes.

6 MEASURMENTS OF WAVE SPECTRA

Figs 3-8 show a sample of a wave spectral estimates from data obtained in Southampton Water. This particular set of data has been used as illustration of each of the analysis methods mentioned in the previous section of this report.

6.1 Frequency Spectra from Power Spectral Density of Acceleration Data (method (a))

Fig 3 shows the result of estimating the power spectral density of the buoy vertical acceleration and its subsequent transformation to a displacement spectral density (method (a) of the previous section). For comparison purposes, a standard ITTC two parameter wave spectrum has been superimposed on both spectral density distributions. The parameters for the ITTC spectrum were chosen to match the zero crossing period and significant height of the measured spectrum. In comparison to the ITTC spectrum, the measured amplitude spectrum lacks the energy peak at the modal frequency and is substantially flat up to 0.5 hz. Beyond this frequency there is slightly more energy than expected from the ITTC spectrum. This characteristic of the amplitude spectrum is less evident in the acceleration spectrum, which seems to follow fairly well the form of the ITTC spectrum. It should be born in mind that it is the acceleration spectrum that is derived directly from the buoy measurements and that conversion to the amplitude spectrum involves division by ω^2. At the low frequencies there is only a small acceleration to measure and scatter in the experiment data can easily dominate the estimated amplitude spectrum. With this in mind the measured wave spectra look very plausible. It should be noted that the buoy acceleration spectrum and the wave slope spectrum have similar forms.

For the record, the wave spectra have been derived from a record of 2048 points digitised at a sample rate of 10 hz. In order to smooth the data, the calculated power spectral components were aggregated into frequency bands of 0.05 hz each containing the sum of approximately

10 components.

6.2 The estimation of spectral directional properties (methods (b) and (c))

Attempts to obtain further details of the wave, including directional properties, have been based on FFT of the of the auto- and cross-correlations of buoy heave, pitch and roll signals. For the wave record used in this report the auto-correlations are shown in Fig 4a, 4b, 4c. The cross-correlations are complex and have not been plotted.

Frequency Spectra estimated by analysis methods (b) and (c), from the auto-correlation of buoy heave via equation (A2.7a), produced results identical to those shown in Fig 3 based on the power spectrum of heave acceleration.

Satisfactory identification of the mean wave direction and the directional spreading function from equations (A2.7d) & (A2.7e) depend on the phase relations between heave, pitch and roll. Identification of these relations from buoy calibration data has proved unobtainable and reliance had to be placed on the assumption that wave slope/pitch and wave slope/roll phase relationships were likely to be the same.

The cross-correlations of pitch/heave and roll/heave are given by equations (A2.7d) and (A2.7e) respectively:

$$A_{1,0,n} = \frac{i}{2} P(\omega_n)\overline{H(\omega_n)} k_n S(\omega_n) \cos\mu_n \int_{-\pi}^{\pi} D_n(\vartheta') \cos\vartheta' d\vartheta' \delta\omega_n \qquad \ldots(A2.7d)$$

and

$$A_{2,0,n} = \frac{i}{2} R(\omega_n)\overline{H(\omega_n)} k_n S(\omega_n) \sin\mu_n \int_{-\pi}^{\pi} D_n(\vartheta') \cos\vartheta' d\vartheta' \delta\omega_n . \qquad \ldots(A2.7e)$$

Dividing equation (A2.7e)by equation (A2.7d) gives

$$\frac{A_{2,0,n}}{A_{1,0,n}} = \frac{R(\omega_n)}{P(\omega_n)} \bullet \tan(\mu_n)$$

Since $R(\omega_n)$ and $P(\omega_n)$ are complex transfer functions for roll and pitch, respectively, the result of this division is complex and the argument is the phase difference between pitch and roll. Fig 5 shows this phase difference as a function of component wave frequency. Up to about 1.0 hz the difference is small (up to about 10 degrees), above 1.0 hz the difference becomes rather erratic. The smallness of this phase difference justifies the use of a working assumption that wave slope/pitch and wave slope/roll responses have the same phase.

Assuming, further, that the amplitudes of $R(\omega_n)$ and $P(\omega_n)$ should be identical, $\tan(\mu_n)$ can be estimated from the modulus of $A_{2.0.n} / A_{1.0.n}$. Fig 6 shows values of μ_n estimated by this method. For the particular wave data analysed in this report the mean wave direction appears to be between 50 and 70 degrees to the buoy axis for component waves up to 1.0 hz and to vary erratically above that frequency. Visual observation at the time indicated a mean wave direction close to the buoy axis. A 60 degree error in estimation of wave heading could arise if the accelerometer channels had been miss-identified when recording the wave data. Efforts to investigate this possibility by cyclically interchanging the accelerometer data channels were not successful.

The auto-correlations for heave, pitch and roll are given by equations (A2.7a),(A2.7b) and (A2.7c) respectively:

$$A_{0,0,n} = \frac{1}{2} H(\omega_n)\overline{H(\omega_n)}S(\omega_n)\delta\omega_n \qquad \ldots(A2.7a)$$

$$A_{1,1,n} = \frac{1}{4} P(\omega_n)\overline{P(\omega_n)}k_n^2 S(\omega_n)\{1+\cos(2\mu_n)\int_{-\pi}^{\pi} D_n(\vartheta')\cos(2\vartheta')d\vartheta'\}\delta\omega_n \qquad \ldots(A2.7b)$$

$$A_{2,2,n} = \frac{1}{4} R(\omega_n)\overline{R(\omega_n)}k_n^2 S(\omega_n)\{1-\cos(2\mu_n)\int_{-\pi}^{\pi} D_n(\vartheta')\cos(2\vartheta')d\vartheta'\}\delta\omega_n \qquad \ldots(A2.7c)$$

If it is assumed that $|H(\omega_n)| = 1.0$ and that μ_n and the spreading function integrals $I_n = \int_{-\pi}^{\pi} D_n(\vartheta')\cos(2\vartheta')d\vartheta'$ are constants, the values of $\sqrt{A_{1,1,n} / k_n^2 A_{0,0,n}}$ and $\sqrt{A_{2,2,n} / k_n^2 A_{0,0,n}}$ are proportional to pitch and roll amplitude transfer functions. The similarity between these quantities and the buoy calibration data is shown in Fig 7. Fig 7a compares $\sqrt{A_{1,1,n} / k_n^2 A_{0,0,n}}$ with the pitch calibration data including the raw calibration data and smoothed calibration data frequency shifted by 0.1 hz to a lower frequency range. Fig 7b compares $\sqrt{A_{2,2,n} / k_n^2 A_{0,0,n}}$ with the raw roll calibration data. Qualitatively the comparison is quite good. It serves show that the buoy calibration data for pitch and roll, although varying with frequency in a totally unexpected way, is probably correct.

The final step in the analysis of directional properties is to take the estimate of μ_n and to estimate the value of the spreading function integral I_n from equations (A2.7b) and (A2.7c). the result is shown in Fig 8. According to Appendix 2, a spreading function of the form $D(\vartheta') = a\cos^{2p}(\vartheta')$ leads to the conclusion that $I_n = \frac{p}{p+1}$. From this result I_n has a value 0.5 for $p = 1$ and increases towards 1.0 as p becomes larger, or as the wave system becomes

unidirectional. In Fig. 8 I_n is approximately 1.0 at low frequencies, but above 1.0 hz the values erratic and not very plausible. On the face of it, this suggests a long crested wave system. However, this conflicts with visual impressions at the time of recording the wave data. It is possible that, although each wave frequency is long crested, individual frequencies vary in direction (since μ_n varies) and that this produced the short crested appearance of the wave system. This interpretation is not totally convincing. The analysis presented here assumed that the transfer functions for buoy roll and pitch have the same amplitude. Attempts to improve results by assuming a ratio of roll response to pitch response less than 1.0 did not significantly change the result. Neither did the use of a mean value of μ_n for all frequencies, nor did the reanalysis of the data using a fixed mean buoy heading rather than allowing for the modulation due to buoy yaw motion.

As noted earlier for the wave spectra, the FFT's of the auto- and cross-correlation functions have been derived from a record of 2048 points digitised at a sample rate of 10 hz. In order to smooth the data, the calculated power spectral components were aggregated into frequency bands of 0.05 hz each containing the sum of approximately 10 components.

7 CONCLUSIONS

7.1 A simple wave buoy has been constructed and instrumented in an inexpensive manner.

7.2 The buoy has been calibrated in heave, pitch and roll in the Lamont tank at the University of Southampton over a limited range of wave frequencies.

7.3 Heave calibration is as expected and satisfactory, although further calibration at lower frequencies is still required. Heave transfer functions are close to unity at low frequencies and fall off at frequencies above 1.0 hz.

7.4 Pitch and roll calibrations show unexpectedly high output at low wave frequencies in a manner similar to the output of pitch and roll in random waves in open water. Clearly the transfer functions for pitch and roll motions relative to wave slope must approach unity as wave frequency approaches zero. The failure of buoy output to behave in this manner requires further investigation.

7.5 The buoy has been deployed in Southampton Water to measure wave spectra in conjunction with motions experiments on a large model catamaran. The buoy deployed directly to windward of the support boat at the end of an extended, but not taut, umbilical cable. During the period of wave measurement the buoy yawed slowly. It was found that, in most cases, the wind direction was a good indication of the mean wave direction.

7.6 One dimensional frequency spectra for the measured waves derived from records taken over a 200 second period proved to be satisfactory. The estimated spectra compared well with standard ITTC two parameter spectra and gave a significant wave heights in

line with a visual estimate made during measurement.

7.7 Estimates of mean wave direction and directional spread have been made based on FFT of auto- and cross-correlations of wave buoy heave, pitch and roll output. Theses estimates rested on assumptions regarding the phase relationships between buoy pitch and roll and the assumption of unity heave response. Results are encouraging but not yet satisfactory and further work is needed in this area.

7.8 In practice, wave conditions vary during the course of a test period of 4 to 5 hours duration. It is not totally satisfactory to measure wave conditions occasionally during this period. Ways to monitor wave conditions during each model test run need exploring.

ACKNOWLEDGEMENTS

The work described in this report covers part of the Fast Craft Research Programme funded by the EPSRC and Industry and managed by Marinetech South Ltd.

REFERENCES

1. Wellicome, J.F., Temarel, P., Molland, A.F., Cic, J. and Taunton, D.J. Experimental measurements of the seakeeping characteristics of fast displacement catamarans in oblique waves. University of Southampton, Ship Science Report No. 111, 1999.

2. Wellicome, J.F., Temarel, P., Molland, A.F., Cic, J. and Taunton, D.J. Experimental measurements of the seakeeping characteristics of a 4.5m fast displacement catamaran in open irregular seas. University of Southampton, Ship Science Report No. 118, 1999.

freq	heave	pitch	freq.	roll
hz	tf	tf	hz	tf
0.565	0.91315	3.72756	0.3906	7.71148
0.5988	0.86616	2.66281	0.46875	3.64491
0.625	1.1552	3.27708	0.5469	2.32544
0.6667	1.01675	2.21295	0.625	1.62536
0.6757	0.98619	2.07468	0.70313	1.16275
0.7194	1.04069	1.63125	0.78	0.74653
0.833	1.02596	1.15993	0.859	1.15993
0.9091	1.00587	1.15332	0.9375	1.15332
0.9901	0.96166	1.13454	1.016	1.13454
1.11	0.86631	0.94961	1.094	0.94961

Table 1. Buoy calibration data

APPENDICES

APPENDIX 1: ESTIMATION OF BUOY MOTIONS RELATIVE TO DATUM DIRECTIONS BASED ON COMPASS ZERO HEADING

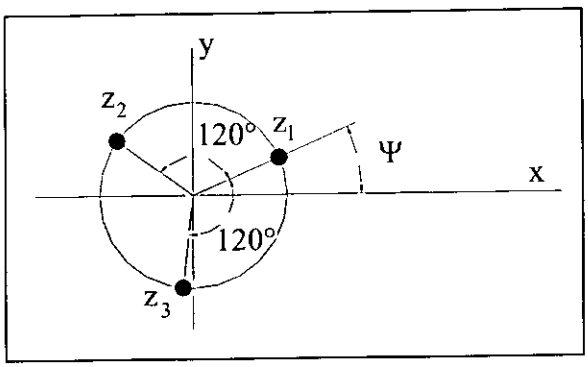

z_1, z_2, z_3 ... Accelerometer vertical displacements

x, y ...Reference axes for wave buoy defining the roll and pitch axes

Ψ ... Wave buoy yaw angle from compass zero heading

r ... Radius of accelerometers from buoy centre

In terms of the heave displacement at the centre of the buoy (z), the roll angle about the x axis (ϕ) and the pitch angle about the y axis (ϑ), the vertical displacements of the accelerometers are given by:

$$z_1 = z - r\vartheta\cos\psi + r\phi\sin\psi \qquad \text{....(A1.1)}$$

$$z_2 = z - r\vartheta\cos(\psi + 120) + r\phi\sin(\psi + 120) \qquad \text{....(A1.2)}$$

and

$$z_3 = z - r\vartheta\cos(\psi - 120) + r\phi\sin(\psi - 120) \qquad \text{....(A1.3)}$$

From these equations :

$$z_2 + z_3 = 2z + r\vartheta\cos\psi - r\phi\sin\psi$$

and

$$z_2 - z_3 = \sqrt{3}r\vartheta\cos\psi + \sqrt{3}r\phi\sin\psi$$

It follows that the buoy attitude is given by:

Heave displacement $z = (z_1 + z_2 + z_3)/3$ ....(A1.4)

Roll displacement $\phi = B\cos\psi + A\sin\psi$ ....(A1.5)

and

Pitch displacement $\vartheta = B\sin\psi - A\cos\psi$ ....(A1.6)

where $A = \dfrac{[2z_1 - (z_2 + z_3)]}{3r}$ and $B = \dfrac{(z_2 - z_3)}{\sqrt{3}r}$

Equation (A1.1) can be differentiated to give

$$\ddot{z}_1 = \ddot{z} - r\ddot{\vartheta}\cos\psi + \left\{2r\dot{\vartheta}\,\dot{\psi}\sin\psi + r\vartheta\,\ddot{\psi}\,\sin\psi + r\vartheta(\dot{\psi})^2\cos\psi\right\}$$
$$+ r\ddot{\phi}\sin\psi + \left\{2r\dot{\phi}\,\dot{\psi}\cos\psi + r\phi\,\ddot{\psi}\cos\psi - r\phi(\dot{\psi})^2\sin\psi\right\}$$

The terms in brackets $\{\ \}$ represent the effects of yaw rate and yaw acceleration on accelerometer acceleration data. If the yaw rate $\dot{\psi}$ and yaw acceleration $\ddot{\psi}$ are sufficiently small, these terms may be neglected. In this case:

$$\ddot{z}_1 = \ddot{z} - r\ddot{\vartheta}\cos\psi + r\ddot{\phi}\sin\psi \qquad \text{....(A1.7)}$$

Similar equations can be found for $\ddot{z}_2$ and $\ddot{z}_3$. It follows that:

$$\ddot{z} = (\ddot{z}_1 + \ddot{z}_2 + \ddot{z}_3)/3 \qquad \text{....(A1.8)}$$

$$\ddot{\phi} = \ddot{B}\cos\psi + \ddot{A}\sin\psi \qquad \text{....(A1.9)}$$

and

$$\ddot{\vartheta} = \ddot{B}\sin\psi - \ddot{A}\cos\psi \qquad \text{....(A1.10)}$$

where $\ddot{A}$ and $\ddot{B}$ follow directly from the earlier definitions of A and B.

This makes it possible to estimate buoy heave, pitch and roll data directly from accelerometer acceleration data without the need to estimate accelerometer displacement data first.

APPENDIX 2: IDENTIFICATION OF WAVE SPECTRAL DETAILS

Equation (1) describes the elevation of the sea surface as:

$$\eta = \sum_{n=0}^{N} \sum_{m} \alpha_{n,m} \cos[k_n x \cos\vartheta_m + k_n y \sin\vartheta_m - \omega_n t + \phi_{n,m}] \quad \ldots(A2.1)$$

This can be rewritten in complex form as:

$$\eta = \sum_{n=-N}^{N} \sum_{m} a_{n,m} e^{i\{k_n x \cos\vartheta_m + k_n y \sin\vartheta_m - \omega_n t\}} \quad \ldots(A2.2)$$

where $a_{n,m} = \frac{1}{2}\alpha_{n,m}\, e^{i\phi_{n,m}}$ for $n > 0$, $a_{-n,m} = \overline{a_{n,m}}$, $k_{-n} = -k_n$ and $\omega_{-n} = -\omega_n$.

This equation can be differentiated with respect to x and y to give expressions for the sea surface slopes in the two principal directions as:

$$\eta_x = \sum_{n=-N}^{N} \sum_{m} ik_n \cos\vartheta_m . a_{n,m} e^{i\{k_n x \cos\vartheta_m + k_n y \sin\vartheta_m - \omega_n t\}} \quad \ldots(A2.3)$$

and

$$\eta_y = \sum_{n=-N}^{N} \sum_{m} ik_n \sin\vartheta_m . a_{n,m} e^{i\{k_n x \cos\vartheta_m + k_n y \sin\vartheta_m - \omega_n t\}} \quad \ldots(A2.4)$$

At the buoy location x=y=0, the buoy responses in heave, pitch and roll can be written as:

$$z_0 = \sum_{n=-N}^{N} \sum_{m} H(\omega_n) . a_{n,m} e^{-i\omega_n t} \quad \ldots(A2.5a)$$

$$z_1 = \sum_{n=-N}^{N} \sum_{m} P(\omega_n) . a_{n,m} e^{-i\omega_n t} \quad \ldots(A2.5b)$$

and

$$z_2 = \sum_{n=-N}^{N} \sum_{m} R(\omega_n).a_{n,m}\, e^{-i\omega_n t} \quad \ldots(A2.5c)$$

In equations (A2.5) $H(\omega_n), P(\omega_n)$ *and* $R(\omega_n)$ are complex transfer functions for buoy heave, pitch and roll responses containing phase as well as amplitude information.

From the buoy motions responses over the time of the wave measurements a series of cross-correlations can be define as:

$$C_{r,s}(t') = Lt_{T\to\infty} \frac{1}{2T} \int_{-T}^{T} z_r(t).z_s(t+t')\,dt \quad \ldots(A2.6)$$

where the suffices r,s take the values 0 for heave, 1 for pitch and 2 for roll respectively.

The Fourier transform of these correlations can be found from the Fourier transforms of the component motions as follows:

On writing $C_{r,s}(t') = \sum_{n=-N}^{N} A_{r,s,n}\, e^{i\omega_n t'}$ and $z_r(t) = \sum_{n=-N}^{N} b_{r,n}\, e^{-i\omega_n t}$ it follows that $A_{r,s,n} = b_{r,n}\overline{b_{s,n}}$.

Assuming that the sea state is spatially uniform and that time averages at the buoy are representative of the sea area as a whole, the transforms of the correlations can be shown to be related to the directional wave spectrum as follows:

$$A_{0,0,n} = \frac{1}{2} H(\omega_n)\overline{H(\omega_n)} S(\omega_n)\delta\omega_n \quad \ldots(A2.7a)$$

$$A_{1,1,n} = \frac{1}{4} P(\omega_n)\overline{P(\omega_n)} k_n^2 S(\omega_n)\{1+\cos(2\mu_n)\int_{-\pi}^{\pi} D_n(\vartheta')\cos(2\vartheta')d\vartheta'\}\delta\omega_n \quad \ldots(A2.7b)$$

$$A_{2,2,n} = \frac{1}{4} R(\omega_n)\overline{R(\omega_n)} k_n^2 S(\omega_n)\{1-\cos(2\mu_n)\int_{-\pi}^{\pi} D_n(\vartheta')\cos(2\vartheta')d\vartheta'\}\delta\omega_n \quad \ldots(A2.7c)$$

$$A_{1,0,n} = \frac{i}{2} P(\omega_n)\overline{H(\omega_n)} k_n S(\omega_n)\cos\mu_n \int_{-\pi}^{\pi} D_n(\vartheta')\cos\vartheta' d\vartheta'\,\delta\omega_n \quad \ldots(A2.7d)$$

and

$$A_{2,0,n} = \frac{i}{2} R(\omega_n)\overline{H(\omega_n)} k_n S(\omega_n)\sin\mu_n \int_{-\pi}^{\pi} D_n(\vartheta')\cos\vartheta' d\vartheta'\,\delta\omega_n . \quad \ldots(A2.7e)$$

In equations (2.7) $S(\omega_n)$ is a one-dimensional frequency spectrum and $D_n(\vartheta')$ is a spreading function and $\vartheta' = \vartheta - \mu_n$ is measured from the mean direction (μ_n) of the wave components of frequency ω_n. $D_n(\vartheta')$ is assumed to be symmetrical about the mean wave direction and a standard representation is taken to be:

$$D(\vartheta') = a\cos^{2p}(\vartheta') \quad : \qquad \frac{-\pi}{2} < \vartheta' < \frac{\pi}{2} \qquad \ldots(\text{A } 2.8)$$

where p is a positive integer.

Integrals of the form $I_q = \int_{-\pi/2}^{\pi/2} \cos^q(\vartheta')d\vartheta'$ can be evaluated as

$$I_{2q} = \frac{\pi(2q)!}{4^q(q!)^2} \qquad \text{and} \qquad I_{2q+1} = \frac{2^{2q+1}(q!)^2}{(2q+1)!}$$

From which $\int_{-\pi/2}^{\pi/2} D_n(\vartheta')d\vartheta' = 1.0$ if $a = \frac{1}{I_{2p}}$

and $\int_{-\pi/2}^{\pi/2} D_n(\vartheta')\cos(2\vartheta')d\vartheta' = \frac{p}{p+1}$.

Finally $\int_{-\pi/2}^{\pi/2} D_n(\vartheta')\cos\vartheta' d\vartheta' = \frac{I_{2p+1}}{I_{2p}}$.

These results make it possible to estimate $S(\omega_n)$ from equation (A2.7a), μ_n from equations (A2.7d) & (A2.7e) and p from equation (A2.7b) or equation (A2.7c).

Estimation of $S(\omega_n)$ is straightforward; satisfactory identification of the mean wave direction and the directional spreading function is more problematical. Equations (A2.7d) & (A2.7e) depend on the phase relations between heave, pitch and roll. Identification of these relations from buoy calibration data has proved unobtainable and reliance had to be placed on the assumption that wave slope/pitch and wave slope/roll phase relationships were likely to be the same. If the mean wave direction is incorrectly identified then the spreading function will not be correctly identified either.

APPENDIX 3: BUOY INSTRUMENTATION

Accelerometers:	Three ICSensor 3145-010 10g range Sensitivity 200mV/g @100Hz 12vDC Supply Resonant frequency 1200Hz Zero acceleration output 2.5 Volts Weight 13 grams
Compass:	CETREK Electronic Compass $\pm 45^{o}$ of heading angle

Data Acquisition:

System 1:	Mowlem ADU TURBOAD
System 2:	Strawberry Tree Data Shuttle DS-16-8-GP-AO 8 Channels AtoD 16 Bit resolution 2Khz Max Speed Dasy*Lab* Data acquisition software

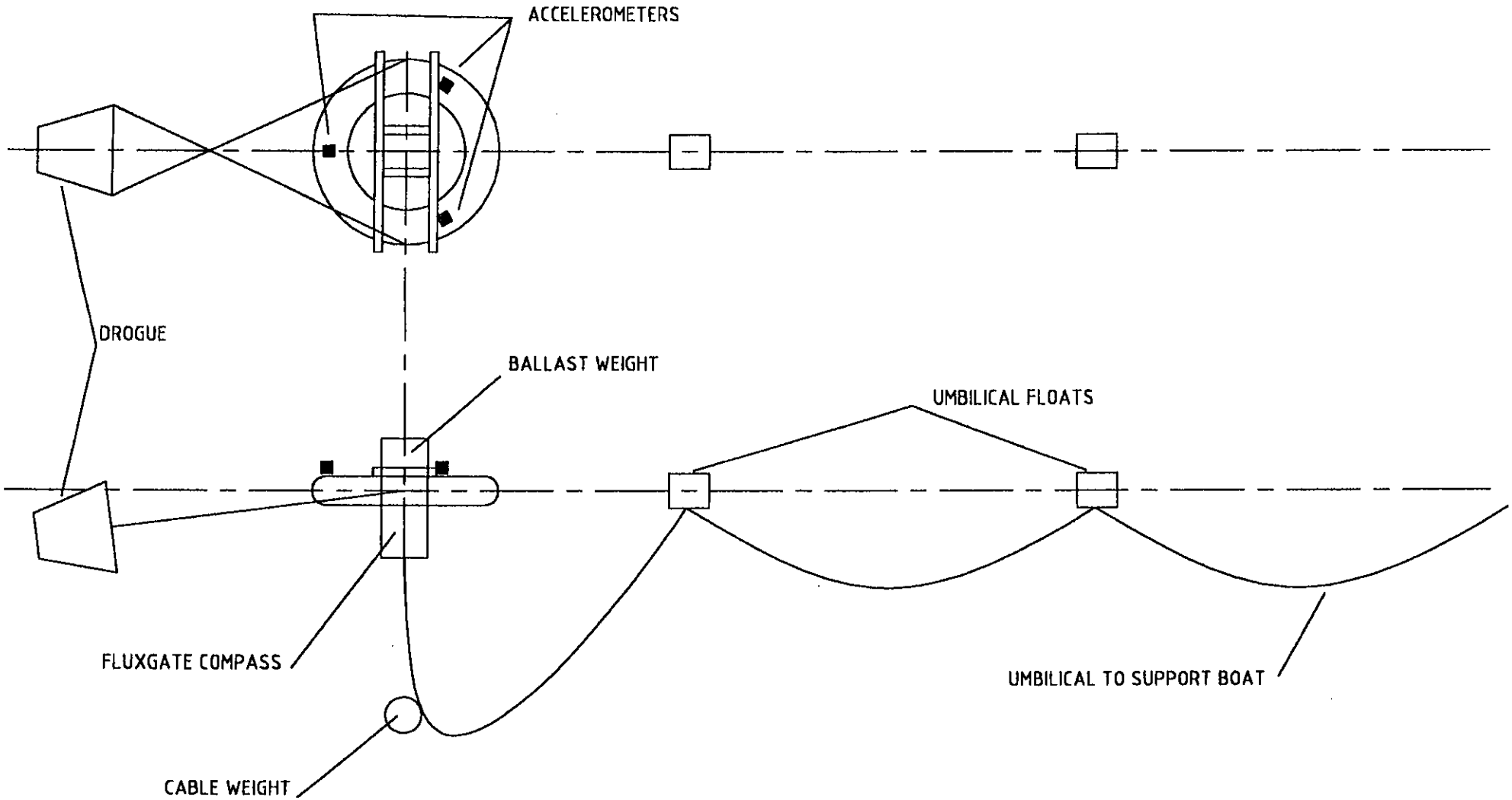

Fig. 1: Wave Buoy Configuration

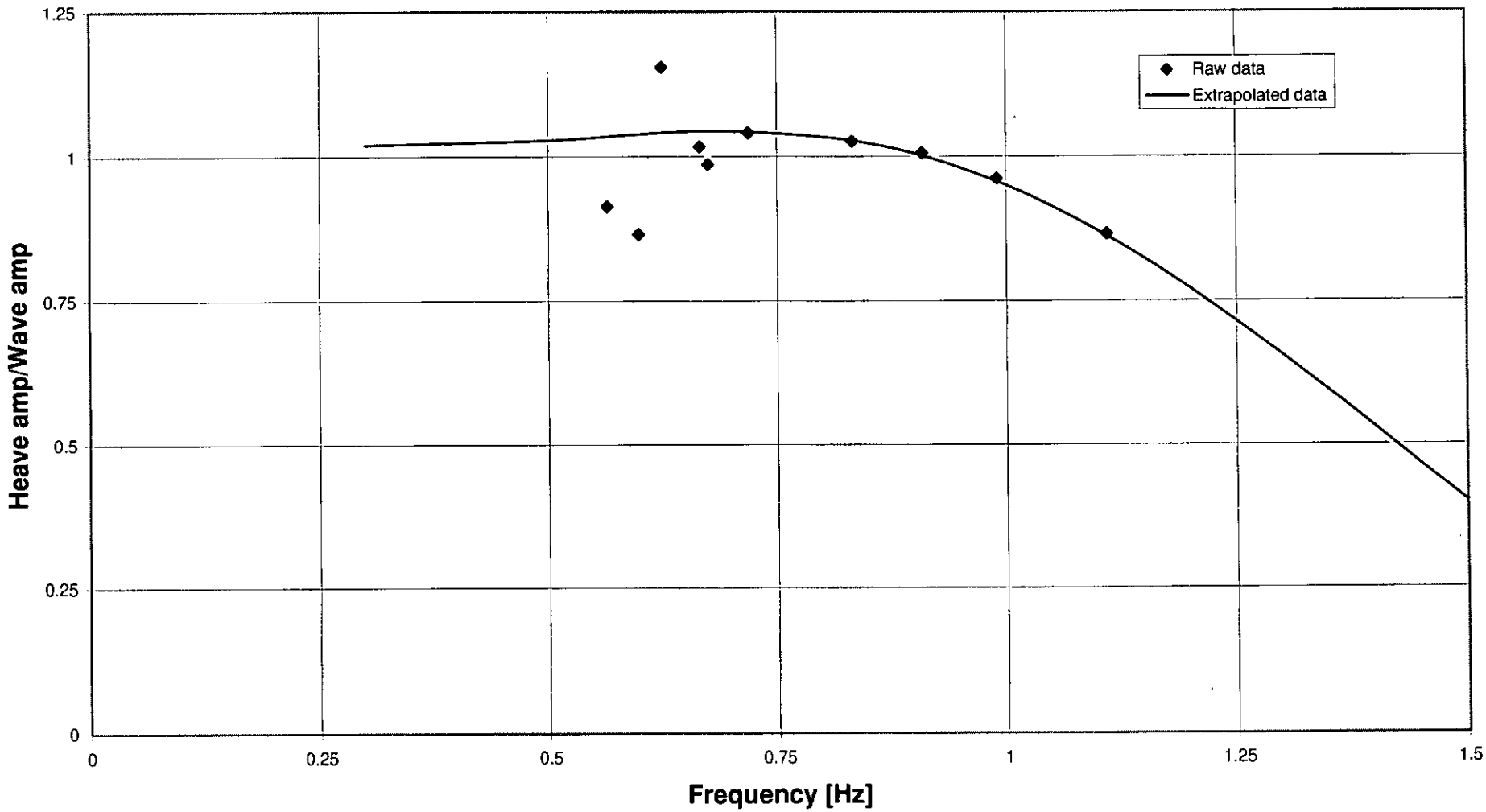

Fig. 2a: Buoy Heave Transfer Function

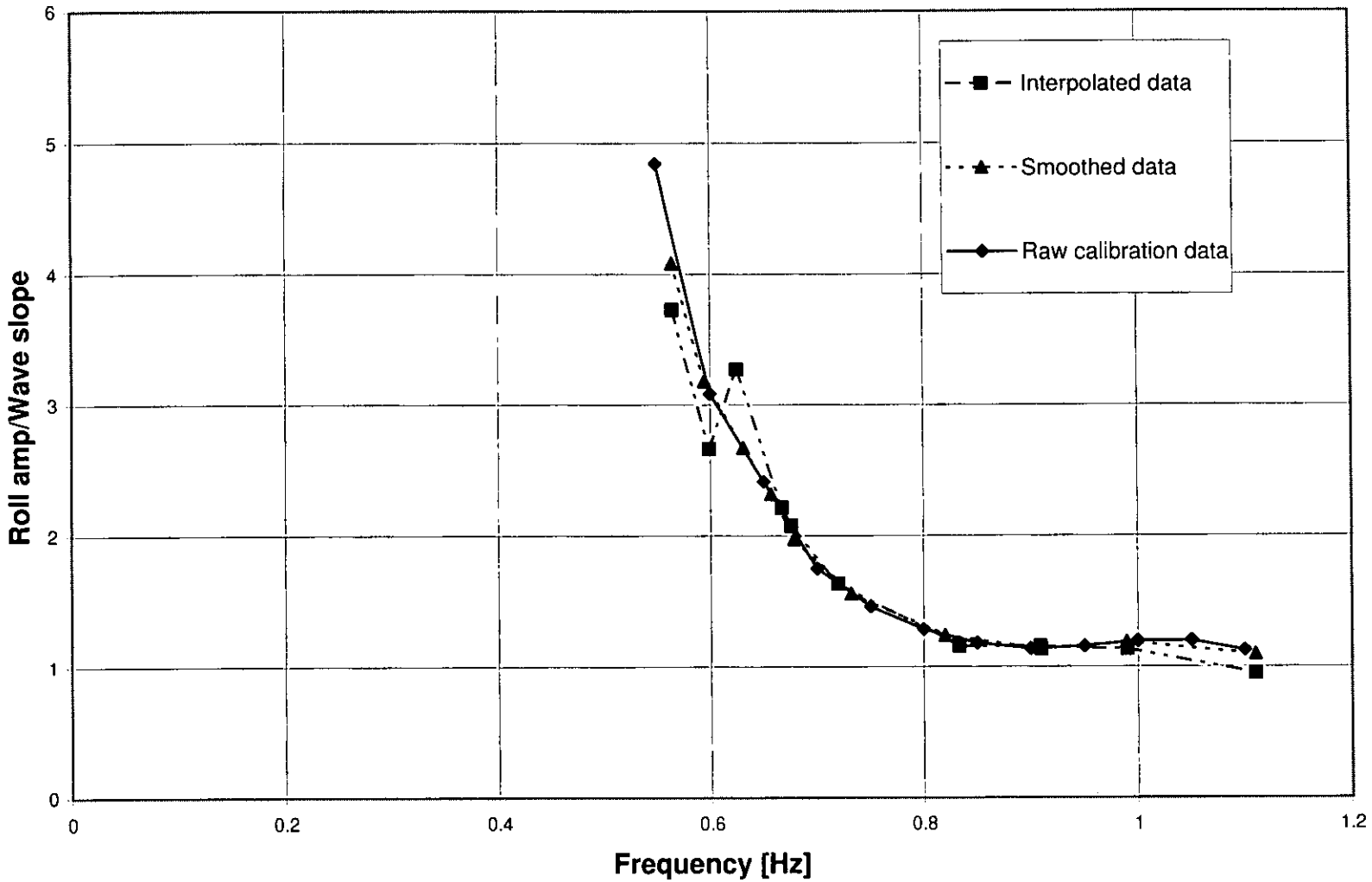

Fig. 2b: Buoy Roll Transfer Function

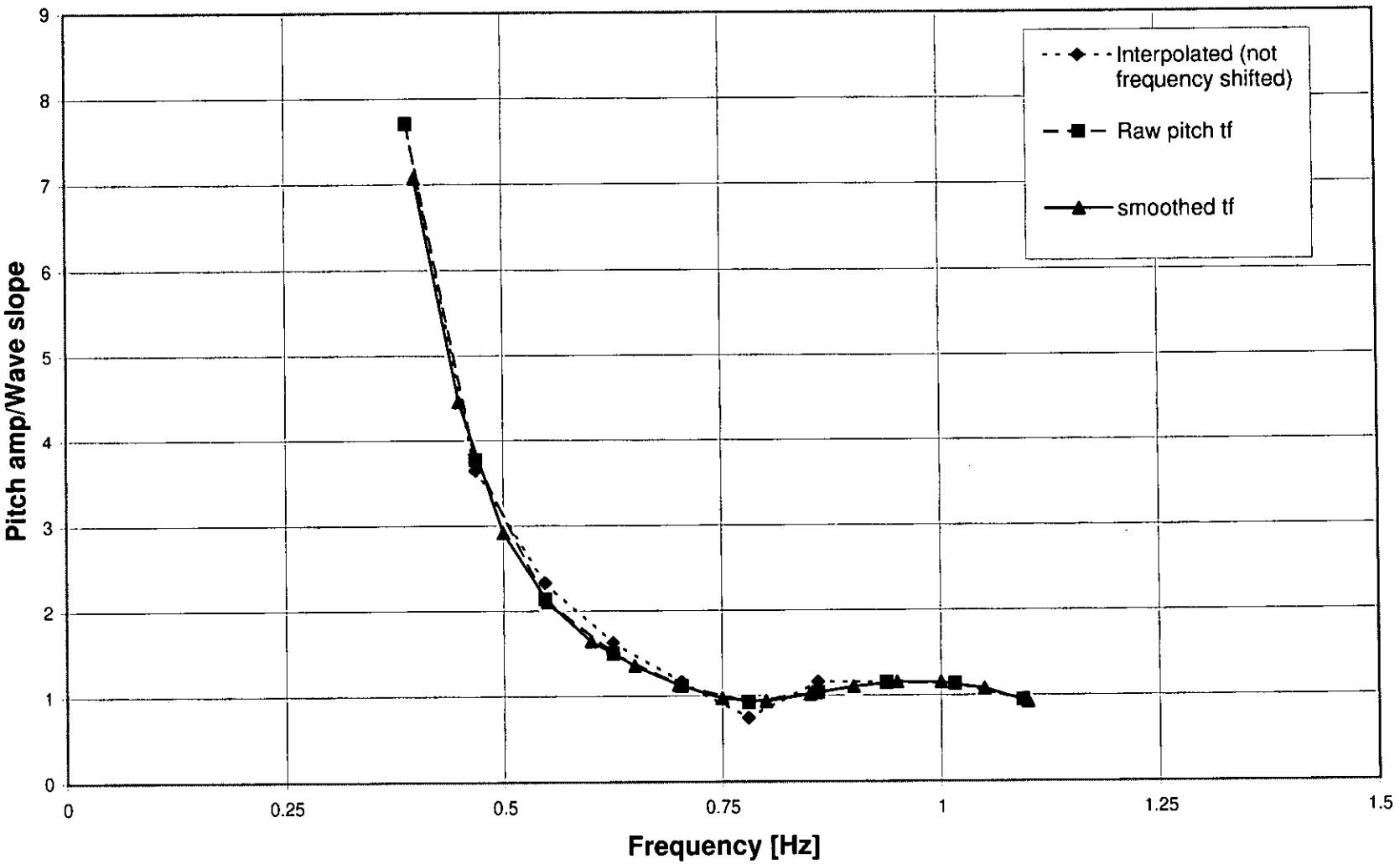

Fig.2c: Buoy Pitch Transfer Function

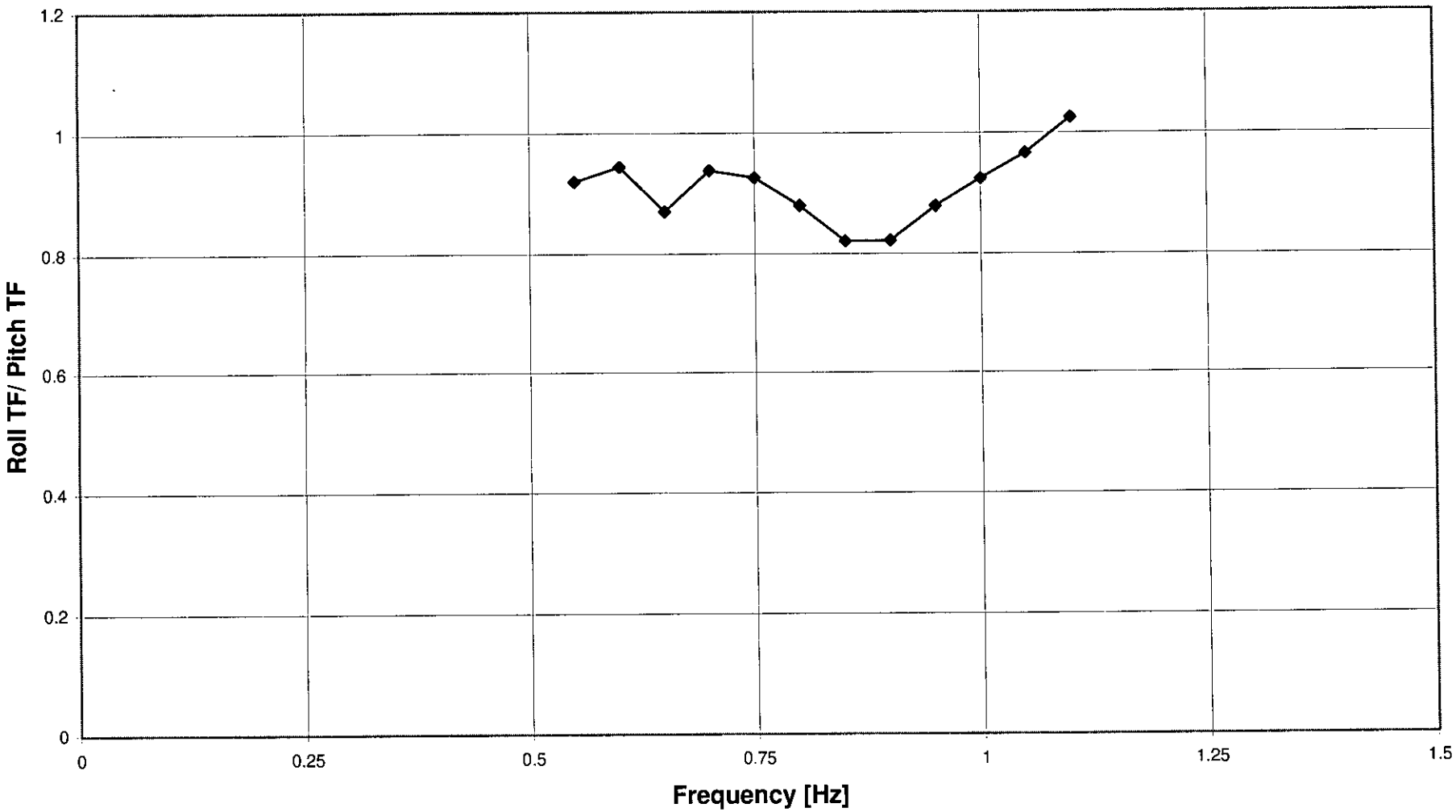

Fig.2d: Buoy Roll TF/ Pitch TF

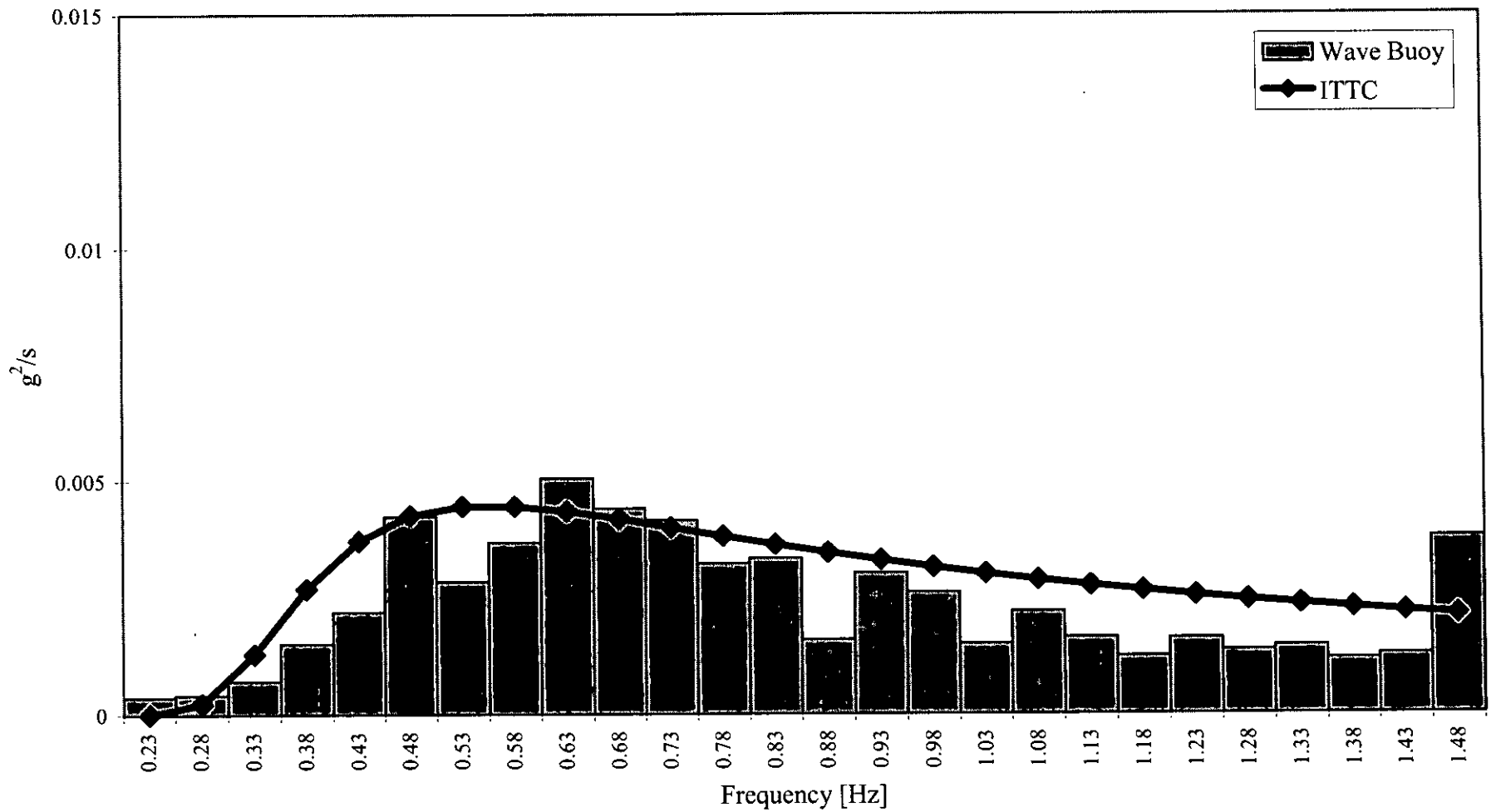

Fig. 3a: Acceleration Spectral Density

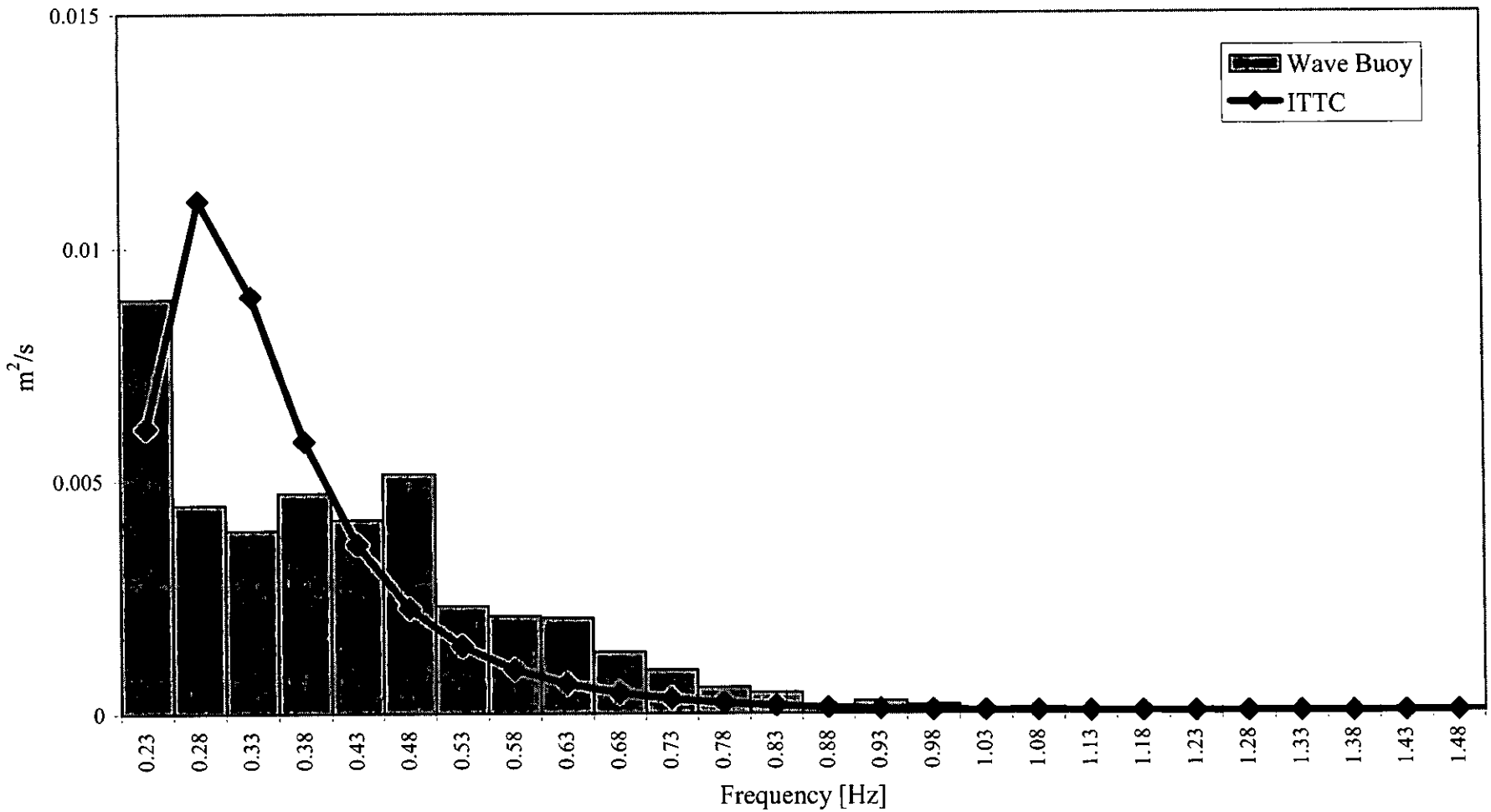

Fig. 3b: Amplitude Spectral Density

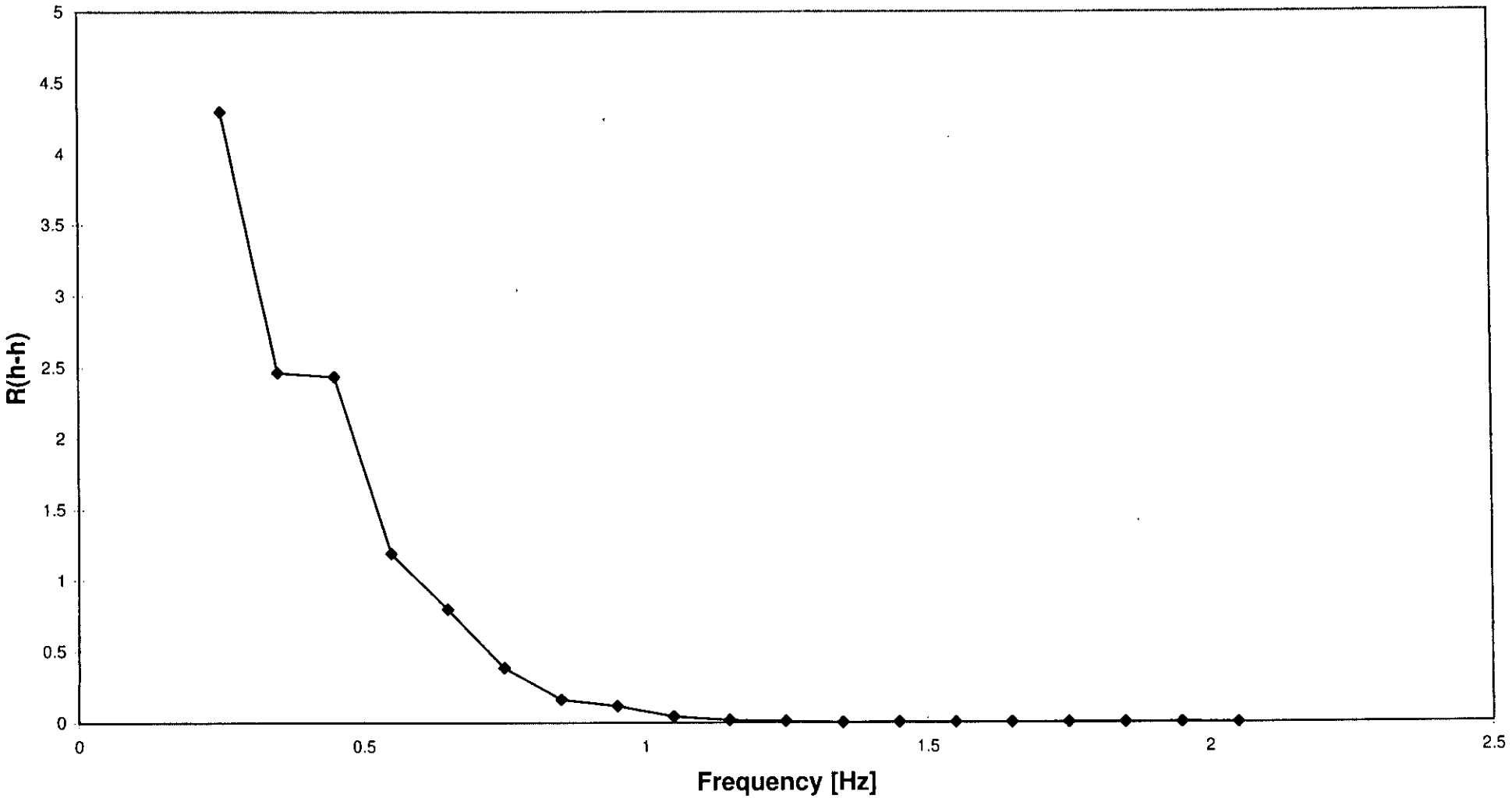

Fig. 4a: Heave auto-correlation

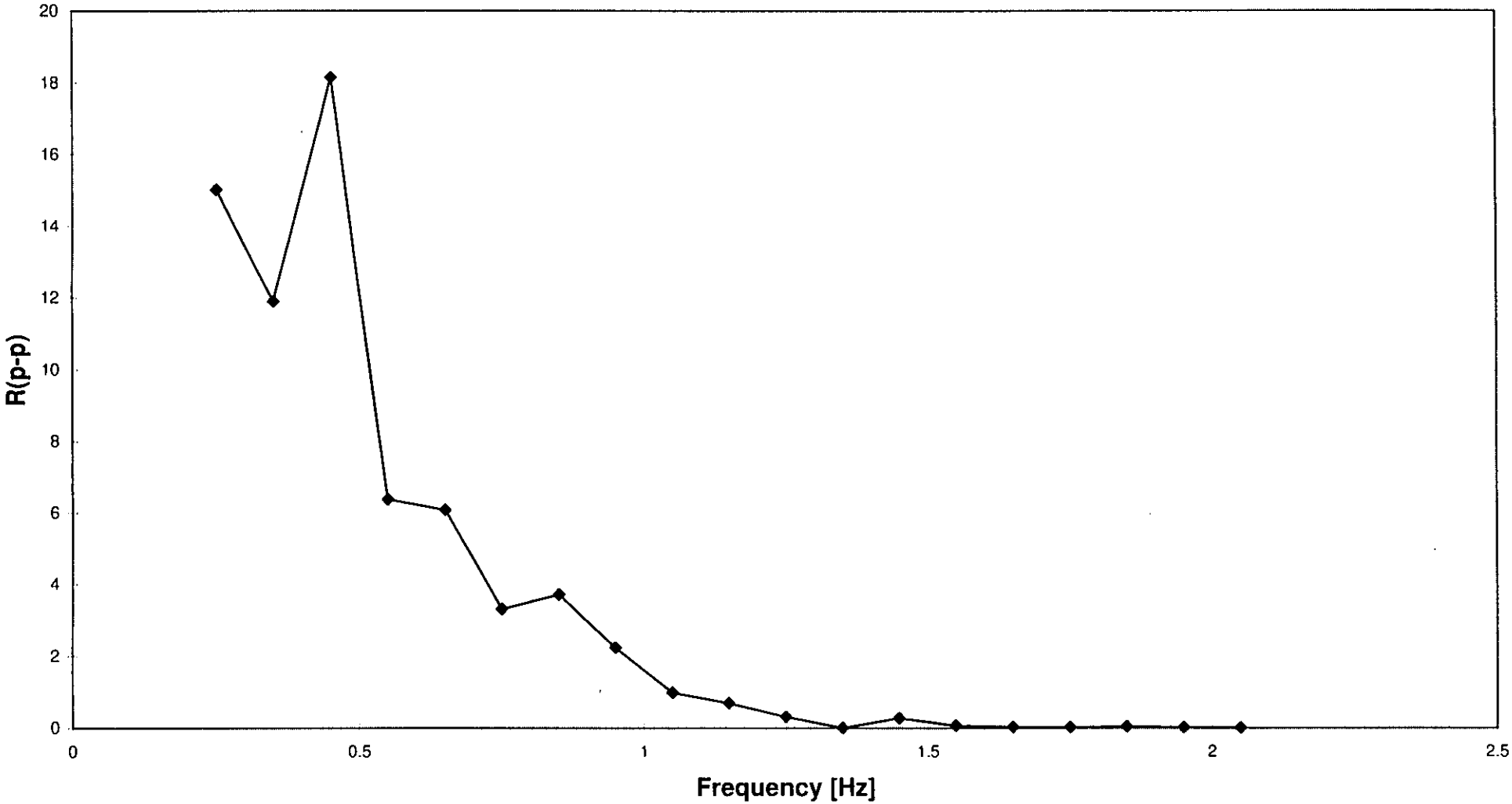

Fig. 4b: Pitch auto-correlation

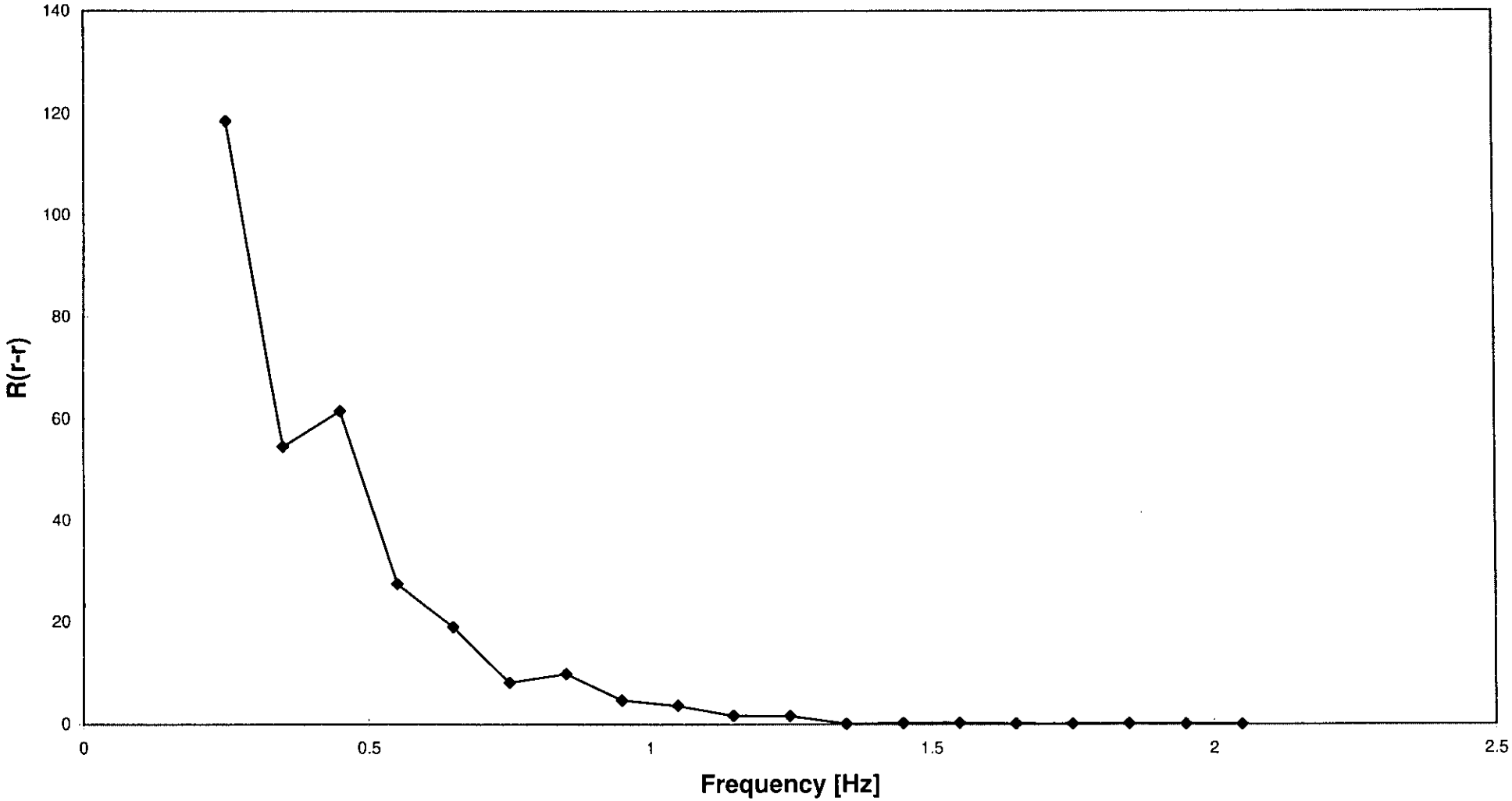

Fig. 4c: Roll auto-correlation

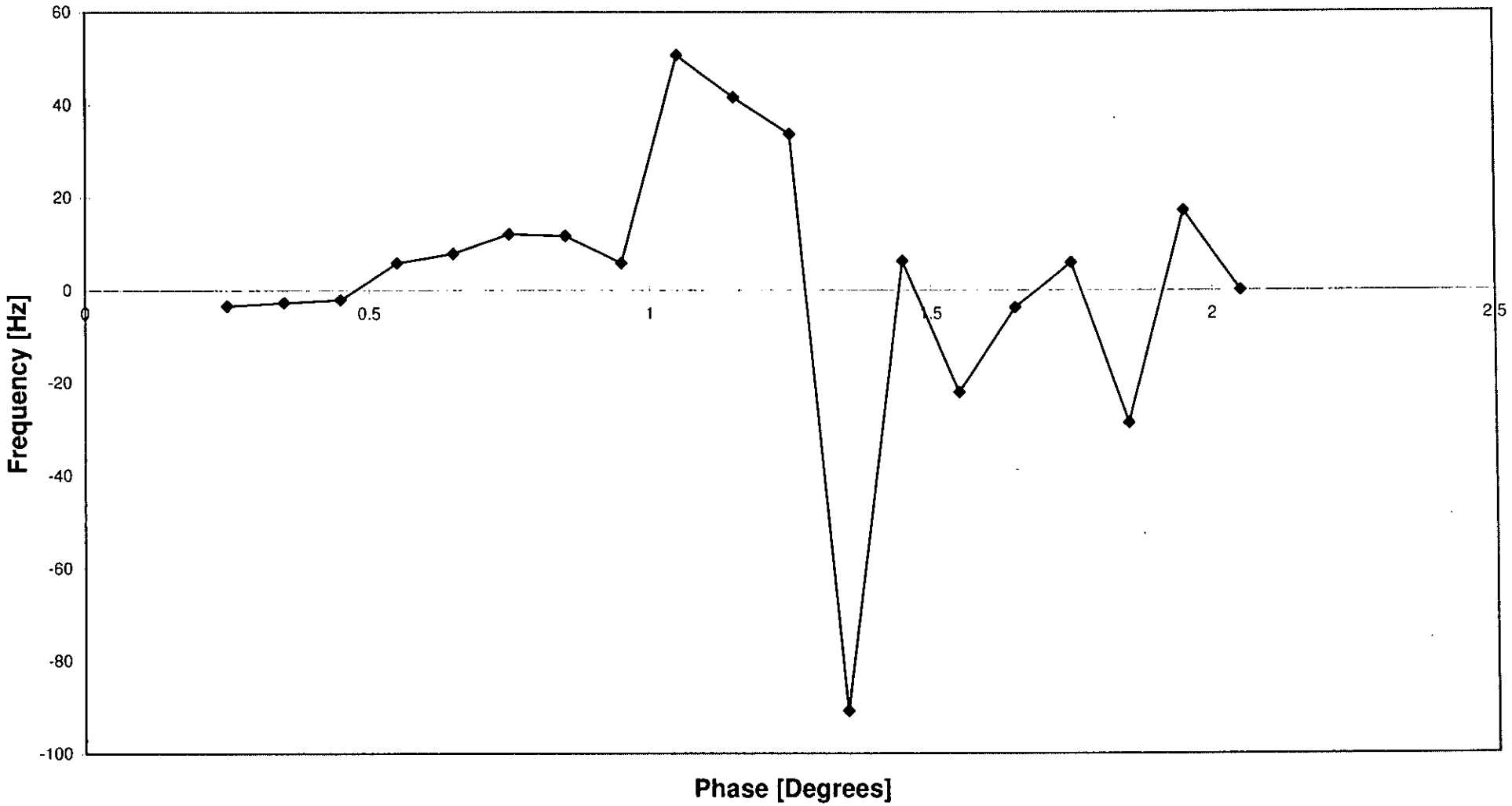

Fig. 5: Roll-Pitch Phase

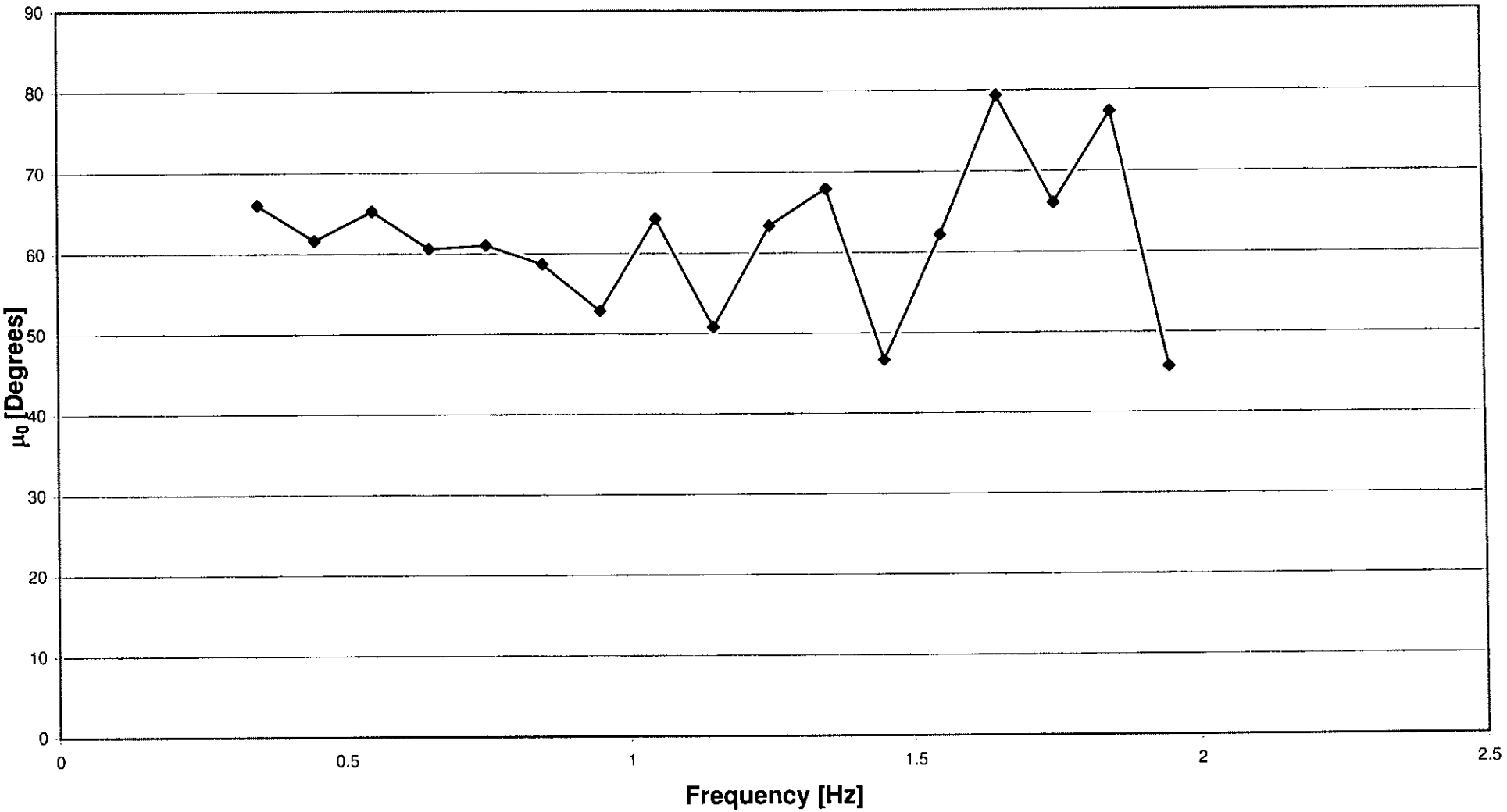

Fig.6: Mean Direction at Each Frequency Band

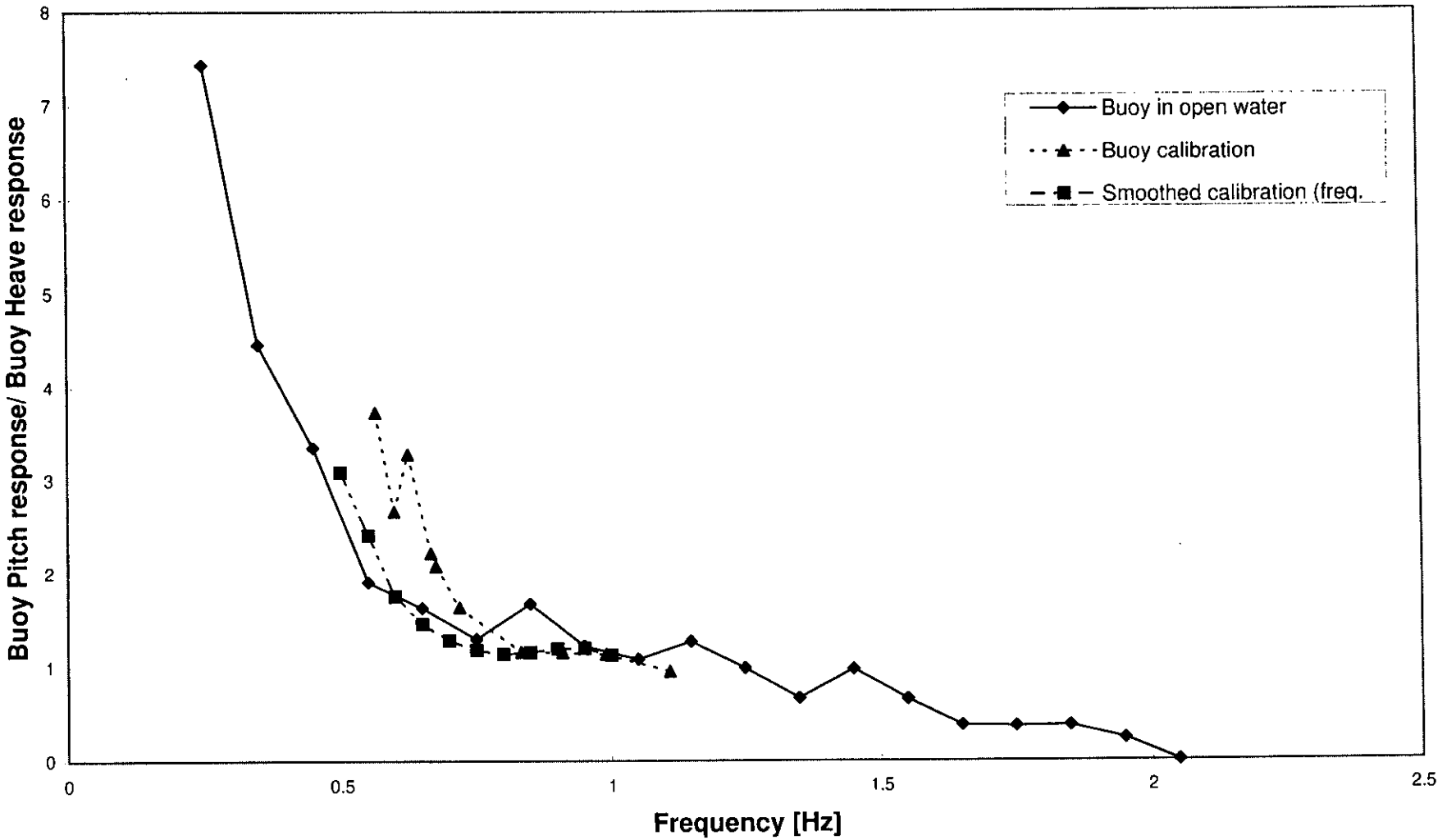

Fig. 7a: Pitch/Heave Amplitude

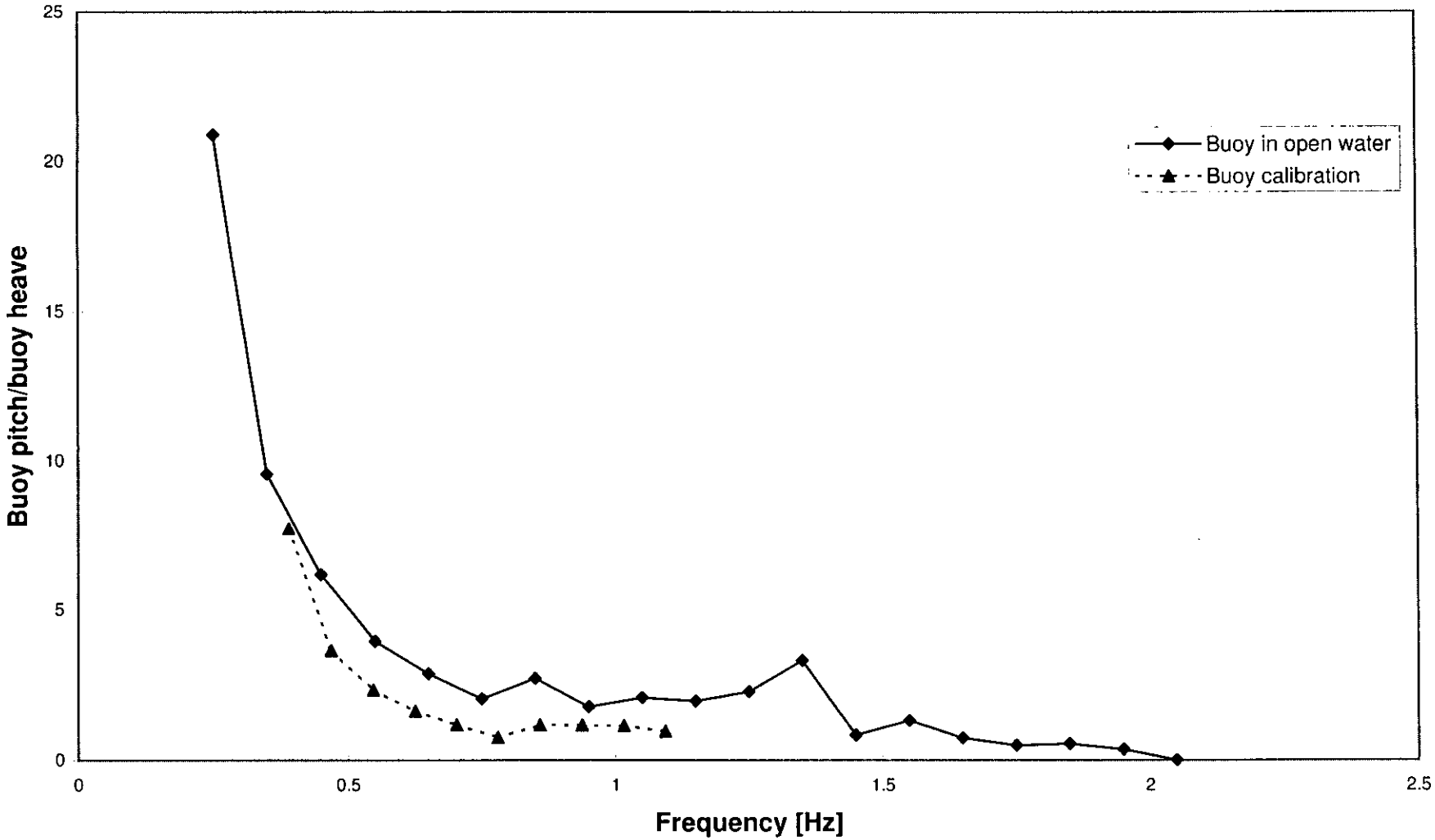

Fig. 7b: Roll/Heave Amplitude

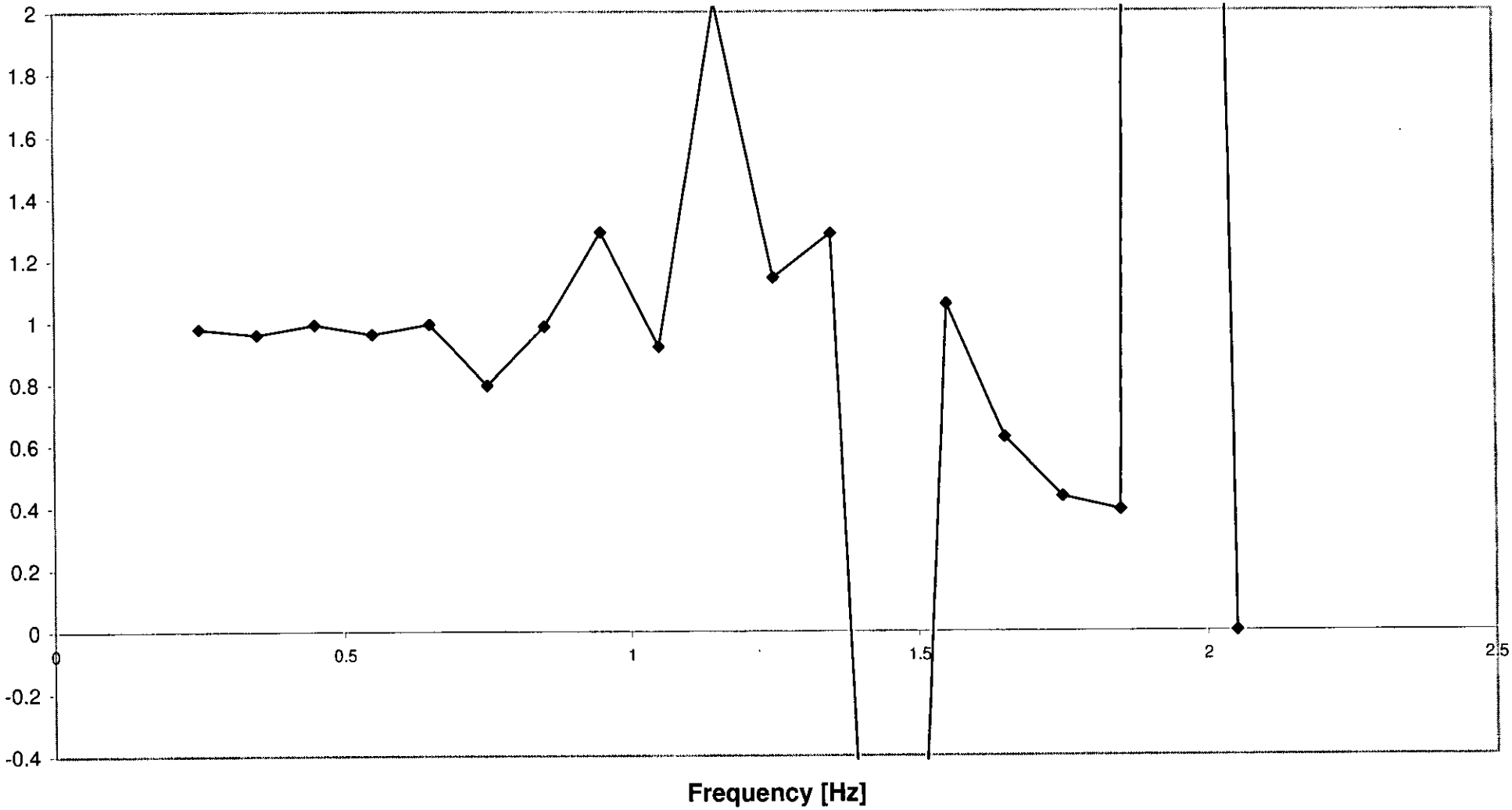

Fig. 8: Spreading Function Integral